Proceedings of the Korean Nuclear Spring Meeting
Gyeongju, Korea, 2004

Fatigue Analysis of Nuclear Welded Structures Using Structural Stress and Fracture Mechanics Approach

Jong-Sung Kim and Tae-Eun Jin
Korea Power Engineering Company
Yongin, Kyunggi-do, Korea

ABSTRACT

The mesh-insensitive structural stress procedure by Dong is modified to apply to the welded joints with local thickness variation and inignorable shear/normal stresses along local discontinuity surface. Validity of the modified mesh-insensitive structural stress procedure is identified comparing the structural stresses calculated for various FE models. Fatigue crack initiation cycles are determined by using the structural stresses and the various fatigue crack growth models. Fatigue test is performed to identify the validity of the fatigue analysis results. Finally, as a result of comparison between test and analysis results, it is found that the structural stress/fracture mechanics approach is valid for fatigue analysis.

1. INTRODUCTION

In nuclear components and structures, almost all pressure boundary fatigue cracks can be initiated at welded joints [1,2]. Therefore, in order to ensure the structural integrity of nuclear welded structures during design life, the fatigue life has to be evaluated by the fatigue (crack initiation) analysis procedures presented in technical codes such as ASME Boiler and Pressure Vessel Code Sec.III [3]. However, the fatigue analysis procedure in ASME B&PV Code Sec.III doesn't explicitly consider the presence of welded joints. Furthermore, a consistent characterization of stress concentration effects due to global/local discontinuities on welded joints can't be readily achieved with a peak stress intensity approach in the fatigue analysis procedure because the peak stress intensities on welded joints with localized stress gradients are actually dependent on mesh sizes/types. Therefore, in order to ensure the reliability of fatigue analysis results via this procedure, the more detailed numerical analysis for mesh sensitiveness of peak stress intensity is performed or the principal stresses from numerical analysis are multiplied by theoretical stress concentration factor (SCF). The former is time-consuming and inefficient approach. For the latter, the multiplication of SCF can ensure the reliability of analysis results because of the conservatism. However, this conservatism can cause the fundamental problem at the design and life extension stage because the need to extend the design life and to consider the light water reactor environmental effect is recently increased. Recently, the various fatigue analysis procedures have been developed in order to reduce the conservatism by erasing the uncertainty of analysis results [4-6].

In the paper, the mesh-insensitive structural stress procedure presented by Dong [4] is partly modified to apply to the specific cases with local thickness variation and inignorable shear/normal stresses along local discontinuity surface. Structural stresses are determined for various finite element models of the welded fatigue test specimen with a semi-circular notch by the modified mesh-insensitive structural stress procedure. Validity of the modified mesh-insensitive structural stress procedure is identified comparing the structural stresses. Fatigue crack initiation cycles are determined by using the structural stress results and the various fatigue crack growth models. Fatigue test is performed to identify the validity of the fatigue analysis results. Finally, as a result of comparison between test and analysis results, it is identified that the structural stress/fracture mechanics approach is valid for fatigue crack initiation analysis.

2. FATIGUE ANALYSIS MODEL

Fig. 1 shows the welded fatigue test specimen with a semi-circular notch located on heat affected zone (HAZ). Fatigue test specimen is made of carbon steels, SA106 Gr.B and ER70S-6. Table 1 presents the welding parameters of this model. Table 2 presents the mechanical/ physical material properties obtained from the indentation method and ASME B&PV Code Sec.II [7]. From Table 2, it is found that specimen is almost even-mismatch. Fig. 2 presents the welding residual stress distributions along the centerline and the tangential line on notch root measured by hole-drilling method. As shown in Fig. 2, it is found that the residual stresses are insignificant.

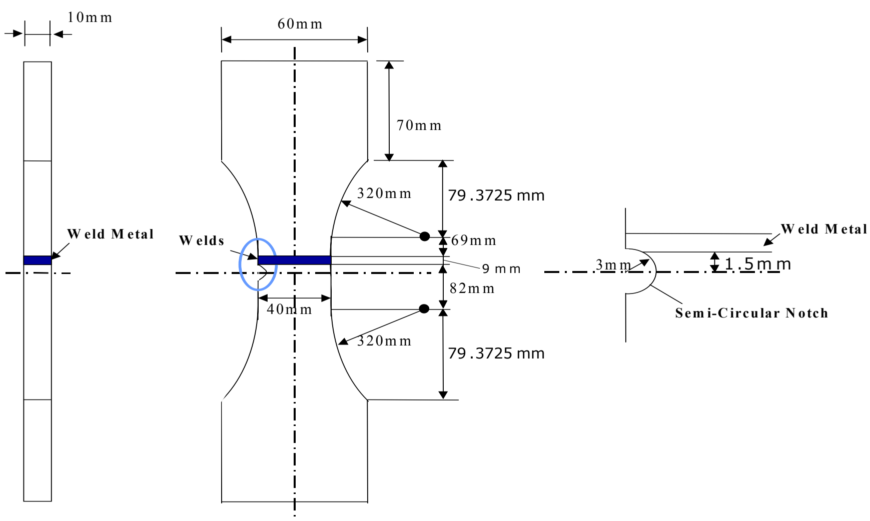

Fig. 1. Configuration of Fatigue Analysis Model.

Table 1. Specification of Welding Parameters

Welding Method	Voltage (V)	Current (A)	Speed (cm/min)	Preheat Temp. (°C)	Interpass Temp. (°C)	PWHT (°C/hr)
GTAW	10~14	100~130	10~13	NA	300 max	610±15/0.5~10.5

Table 2. Mechanical and Physical Material Properties

Elastic Modulus (GPa)	Poisson Ratio	Yield Strength (MPa)			Tensile Strength.(MPa)		
		Base Metal	Weld Metal	Heat Affected Zone	Base Metal	Weld Metal	Heat Affected Zone
203.4	0.3	278.5	282.0	299.3	552.9	541.8	578.7

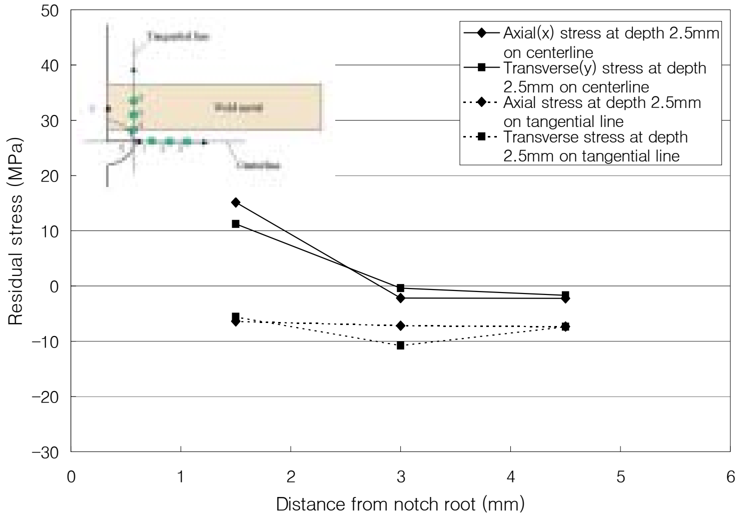

Fig. 2. Welding Residual Stress Distributions along Centerline and Tangential Line on Notch Root

3. MODIFIED MESH-INSENSITIVE STRUCTURAL STRESS PROCEDURE

With a new definition of the structural stress concept, Dong [4] has developed a robust structural stress procedure for analyzing welded joints. As discussed by Dong [4] and Dong et al. [6], a structural stress definition can be stated as follows:

- From the fracture mechanics viewpoint, through-thickness normal stress distribution with respect to the hypothetical crack plane at the weld toe controls the fatigue crack propagation process.
- To ensure mesh-insensitivity, the structural stress σ_s must satisfy equilibrium conditions within the context of elementary structural mechanics theory at the hypothetical crack plane with respect to a reference stress state prescribed by local stresses from typical finite element solutions.
- While local stresses near a notch are mesh-size sensitive due to the asymptotic singularity behavior as approaching at a notch position, the imposition of the equilibrium conditions in the context of elementary structural mechanics within a reference region should eliminate or minimize the mesh-size sensitivity in the structural stress calculations.

The normal structural stress is defined at a location of interest such as Section A-A at the weld toe in Fig. 3 with a plate thickness of t. A second reference plane can be defined along Section B-B in Fig. 3, along which both local normal and shear stresses can be directly obtained from a finite elements solution. By imposing equilibrium conditions between Sections A-A and B-B, the structural stress components, membrane stress σ_m and bending stress σ_b, must satisfy the following conditions:

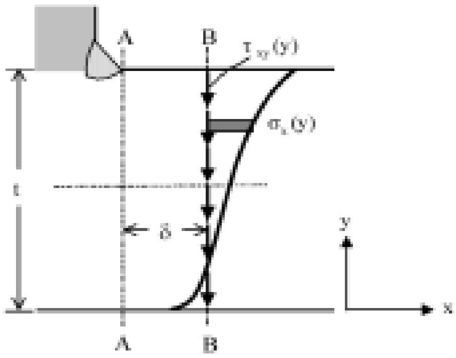

Fig. 3. Structural Stresses Calculation for Through-Thickness Fatigue Crack

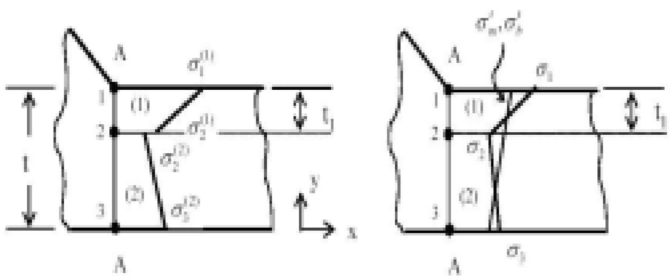

(a) (b)

Fig. 4. Estimation of Partial Thickness Structural Stress

(a) After applying eqs. (1) & (2)

(b) Imposing equilibrium requirements for regions (1) & (2) and continuity at location 2

$$\sigma_m = \frac{1}{t}\int_0^t \sigma_x(y)dy \tag{1}$$

$$\sigma_b \frac{t^2}{2} + \sigma_b \frac{t^2}{6} = \int_0^t \sigma_x(y)ydy + \delta\int_0^t \tau_{xy}(y)dy \tag{2}$$

A fatigue crack of a finite small depth (partial thickness) is used as a final fatigue failure criterion in performing fatigue crack initiation testing [8.9]. In addition, the self-equilibrating part of the stress distribution shown in Fig. 3 requires the consideration of equilibrium conditions within a characteristics distance t_1. As shown in Fig. 4, by applying eqs. (1) and (2) separately in regions (1) and (2), the normal stresses $\sigma_1^{(1)}$, $\sigma_2^{(1)}$, $\sigma_2^{(2)}$, and $\sigma_3^{(2)}$ can be calculated. By enforcing equilibrium conditions and traction continuity at position 2, as shown in Fig. 4(b), the following equations are obtained:

$$\sigma_1 = \frac{1}{2}(2\sigma_1^{(1)} + \sigma_2^{(1)} - \sigma_2^{(2)}) - \frac{t_1}{2t}(\sigma_2^{(1)} - \sigma_2^{(2)})$$

$$\sigma_2 = 2\sigma_2^{(2)} + \frac{t_1}{t}(\sigma_2^{(1)} - \sigma_2^{(2)}) \tag{3}$$

$$\sigma_3 = \sigma_3^{(2)} + \frac{t_1}{2t}(\sigma_2^{(2)} - \sigma_2^{(1)})$$

The equivalent membrane and bending components within regions (1) and (2) are determined as follows:

$$\sigma_m = \frac{\sigma_1 + \sigma_2}{2}, \quad \sigma_b = \frac{\sigma_1 - \sigma_2}{2}, \quad \sigma'_m = \frac{\sigma_2 + \sigma_3}{2}, \quad \sigma'_b = \frac{\sigma_2 - \sigma_3}{2} \tag{4}$$

If the inignorable shear/normal stress occurs on local discontinuity surface due to local thickness variation, eqs. (1) and (2) have to be modified in order to consider the effect of shear/normal stresses on equilibrium condition. By imposing equilibrium conditions between Sections A-A and B-B in Fig. 5, the structural stress components within a characteristics distance t_1, $\sigma_m^{(1)}$ and $\sigma_b^{(1)}$, are deter-mined as follows:

$$\sigma_m^{(1)} = \frac{1}{t_1}[\int_{-h}^{t_1} \sigma_x(y)dy - \int_{-\delta}^{0} \tau'_{xy}(y)dy - \int_{-\ell}^{0} \sigma_n(s)ds\cos\theta + \int_{-\ell}^{0} \tau_{ns}(s)ds\sin\theta] \tag{5}$$

$$\sigma_b^{(1)} = \frac{6}{t_1^{\,2}}[-\frac{\sigma_m^{(1)}t^2}{2} + \int_{-h}^{t_1} \sigma_x(y)ydy + \delta\int_{-h}^{t_1} \tau_{xy}(y)dy + \int_{-\delta}^{0} \sigma'_y(x)xdx - t_1\int_{-\delta}^{0} \tau'_{xy}(y)dy - \int_{-\ell}^{0} \sigma_n(s)sds] \tag{6}$$

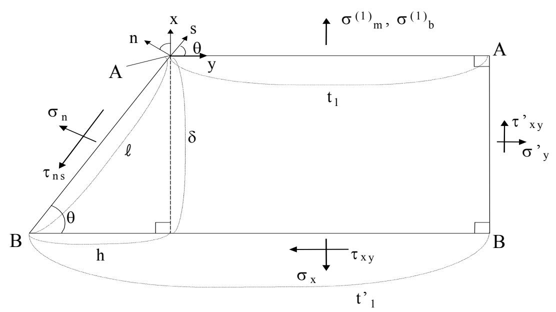

Fig. 5. Structural Stress Calculation Procedure for Local Thickness Variation

3.1 Finite Element Models

An eight-node solid element model is used as shown Fig. 6(a) and 6(b), illustrating two representative meshes with drastically different element sizes at the notch on HAZ. In order to investigate the influence of integration characteristics, the quadratic elements are used with full or reduced integration.

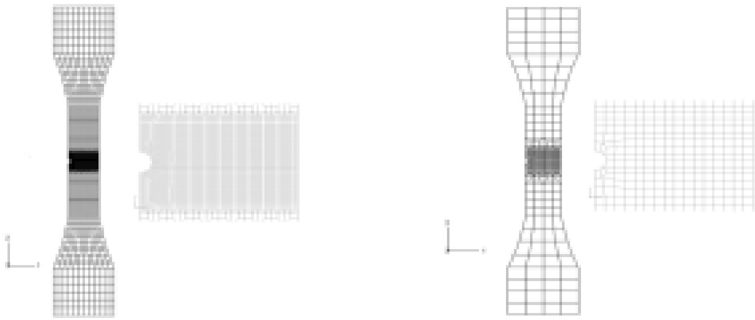

(a) Fine mesh (k=/r=0.2360)   (b) Coarse mesh (k=/r=0.6667)

Fig. 6. Finite Element Mesh for Analysis (r: notch radius)

3.2 Calculation of Structural Stresses

Fig. 7 shows the structural stress based SCF values calculated from the modified structural stress procedure. The SCF values are calculated normalizing the structural stresses obtained from the modified structural stress procedure by remote nominal stress σ_n. As shown in procedure is valid. As a result, it is found that the structural stress calculated from the modified structural stress procedure can serve as an intrinsic stress parameter because of the mesh-size insensitiveness. Fig. 7, it is identified that the modified mesh-insensitive structural stress.

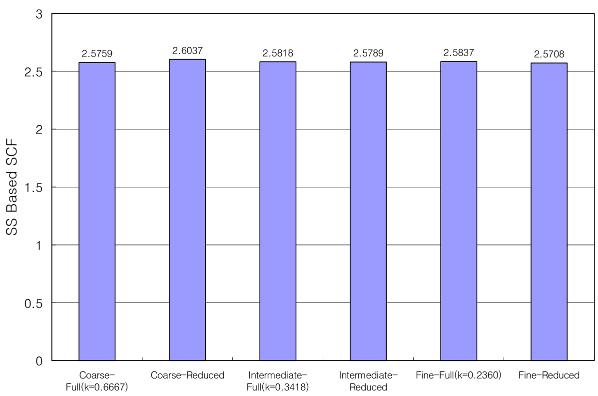

Fig. 7. Structural Stress Based SCF Values for Various FE Models

4. FATIGUE ANALYSIS

The fatigue crack initiation life, defined as the number of cycles required to form an engineering-size small crack, i.e., 3mm deep, is composed of the growth of (a) microstructurally small crack and (b) mechanically small crack [10]. Based on the definition of fatigue crack initiation life, the research that has occurredover the last two decades on "microstructurally small and mechanically small" crack growth has evolved into a new design concept that provides an alternative to the traditional safe-life (or S-N) approach [11]. Therefore, in this study, a fracture mechanics approach is also used to evaluate the fatigue lives of test specimens under strain controlled fatigue loading presented in Table 3.

Table 3. Fatigue Analysis and Test Cases for Welded Specimen with a Semi-Circular Notch under Strain Controlled Fatigue Loading

Case	ε_{max} 1)	ε_{min} 1)	$\Delta\varepsilon$ 2)	R 3)
1	0.00256	0.0000256	0.0025344	0.001
2	0.00156	0.000156	0.001404	0.1
3	0.00076	0.000152	0.000608	0.2

1) ε_{max} and ε_{min} are measured and controlled within the range of gauge length

2) $\Delta\varepsilon = \varepsilon_{max} - \varepsilon_{min}$ 3) $R = \varepsilon_{max} / \varepsilon_{min}$

4.1 Calculation of Stress Intensity Factors

The stress intensity factor (SIF) K can be readily estimated by using the membrane/bending components of structural stress, calculated at a location of interest at anarbitrary weld, as the far-field stress components in the existing K solutions. For 2D specimen with an edge crack, the Mode I SIF K can be expressed as follows [12]:

$$K = \sqrt{t}[\sigma_m^{(1)} f_m(\frac{a}{t}) + \sigma_b^{(1)} f_b(\frac{a}{t})] \tag{7}$$

$$f_m(\frac{a}{t}) = [0.752 + 2.02(\frac{a}{t}) + 0.37(1 - \sin\frac{\pi a}{2t})^3] \cdot \frac{\sqrt{2\tan\frac{\pi a}{2t}}}{\cos\frac{\pi a}{2t}} \tag{8}$$

$$f_b(\frac{a}{t}) = [0.923 + 0.199(1 - \sin\frac{\pi a}{2t})^4] \cdot \frac{\sqrt{2\tan\frac{\pi a}{2t}}}{\cos\frac{\pi a}{2t}} \tag{9}$$

where $\sigma_m^{(1)}$ and $\sigma_b^{(1)}$ are calculated under the assumption that the characteristics distance t_1 is identical to crack depth a.

Fig. 8 presents the variation of normalized SIF for case 1 with crack advance. The normalized SIF is calculated normalizing SIF by nominal SIF $K_n (= \sigma_n \sqrt{\pi a})$.

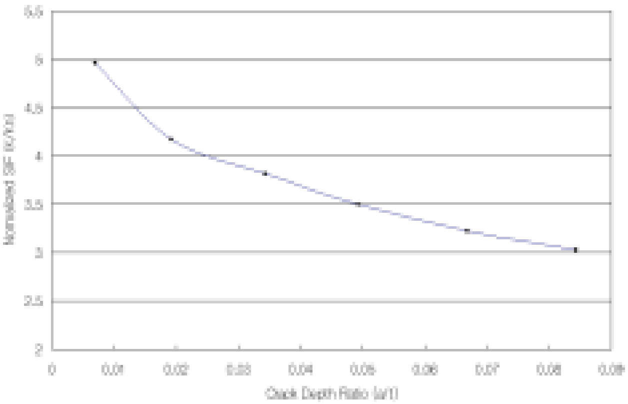

Fig. 8. Variation of Normalized SIF with Crack Advance.

4.2 Initial Crack Size

Tokaji et al. [13, 14] defined crack initiation as the formation of a 10μm deep crack. Gavenda et al. [15] reported that in room temperature air, 10μm deep cracks form early during fatigue life, i.e., <10% of fatigue life. Based on these results, Park and Chopra [10] determined the initial depth of microstructurally small cracks to be 10μm. In this study, it is assumed that the initial crack size is 10μm.

4.3 Transition from Microstructurally Small to Mechanically Small Crack

The previous study results [13,16,17] about transition from microstructurally small to mechanically small crack indicate that crack length for transition depends on applied stress and microstructure; actual value may range from 150 to 250μm. Park and Chopra [10] determined the transition crack depth to be 200μm. Based on these results, it is reasonable to assume the transition crack depth to be 200μm.

4.4 Fatigue Crack Growth Rates

The growth rate da/dN(mm/cycle) of microstructurally small cracks, i.e., from 10 to 200μm, in air can be represented by the Miller's best-fit equation [18] using the Hobson relationship [19].

$$da/dN = 1.475 \times 10^{-35} (\Delta\sigma)^{11.49} (0.3 - a) \quad \text{(carbon steel)} \tag{10}$$

where the stress range $\Delta\sigma$(MPa) is determined considering the elastic structural membrane stress analysis results and tensile strength. Because growth rate increases significantly with decreasing crack lengths a(mm), a constant growth rate is assumed for crack depths smaller than 0.075mm.

The growth rate da/dN(mm/cycle) of mechanically small cracks, i.e., from 200μm to 3mm, in air can be represented by the following relations given in Article A-4300 of ASME B&PV Code Sec.XI [20] and FATDAC [21] respectively:

$$da/dN = 9.73 \times 10^{-8} \left(\frac{\Delta K}{2.88 - R}\right)^{3.07} \quad (0 \le R \le 1,\ \text{carbon steel}) \tag{11}$$

$$da/dN = 7.87 \times 10^{-8} \left(\frac{\Delta K}{2.88 - R}\right)^{3.07} \quad \text{(carbon steel)} \tag{12}$$

where the SIF range ΔK(MPam) is calculated subtracting $K_{\min}$ from $K_{\max}$.

4.5 Estimates of Fatigue Life

Fracture mechanics based prediction of life in cycles to engineering crack depth 3mm can be expressed as follows:

$$N_f = N_{MSC} + N_{MC} \tag{13}$$

$$N_{MSC} = 0.065 \frac{da}{dN}\Big|_{a=0.075} + \int_{0.075}^{0.2} \frac{10^{35} da}{1.475(\Delta\sigma)^{11.49}(0.3 - a)} \tag{14}$$

$$N_{MC} = \int_{0.2}^{3} \frac{10^{8}}{9.73 \ or \ 7.87} \left(\frac{2.88 - R}{\Delta K}\right)^{3.07} da \tag{15}$$

To investigate the basic adequacy ofpresent method based on structural stress and fracture mechanics approach, it is necessary to compare with S-N approach. The current fatigue design curves in ASME B&PV Code Sec.III are based on experimental data on small polished test specimens [22]. The best-fit curve [22] to the experiment-tal data, expressed in terms of strain amplitude ε_a(%) and fatigue cycles N_f, for carbon steel is given by

$$\ln N_f = 6.726 - 2.0 \ln(\varepsilon_a - 0.0722) \tag{16}$$

The strain amplitudecan be calculated from elastic stress analysis results as follows:

$$\varepsilon_a = \frac{S_{alt}}{E} = \frac{K_e S_p}{2E} \qquad (17)$$

where the alternating stress intensity S_{alt} is determined from peak stress intensity range S_p and elastic-plastic strain correction factor K_e.

Table 4 presents the fatigue lives of test specimens predicted by using eqs. (13)~(17). From Table 4, it is found that the fatigue lives predicted via the structural stress/fracture mechanics approach show reasonable agreement with the predicted lives using a best-fit curve in ASME B&PV Code Sec.III. However, the high cycle fatigue lives predicted via the structural stress/fracture mechanics approach seem to be lower and more conservative than the one of ASME best-fit fatigue curve.

Table 4. Fatigue Lives of TestSpecimen Evaluated by Structural Stress/ Fracture Mechanics Approach and ASME B&PV Code

Case	Miller +ASME B&PV Code Sec.XI 1)	Miller +FATDAC 1)	ASME Code Sec.III Best-Fit Curve 2)
1	3244	3345	2349
2	24798	25368	41838
3	452146	458796	2043436

1) Calculated from the structural stresses of the intermediate mesh

2) Calculated from the peak stress intensities of the fine mesh

5. FATIGUE TEST

To identify the validity of fatigue analysis results, the strain controlled fatigue test is performed for the cases presented in Table 3. The tests have been performed three times for each case. Table 5 presents the fatigue lives of test specimens obtained from fatigue test. Fig. 9 shows the ratios of predicted fatigue lives to average test data. Fig. 10 presents the predicted $\triangle\varepsilon$-N_f curves and the test data. From Fig. 9 and 10, it is found that the structural stress/fracture mechanics approach has good agreement with the test results over all cycle regions but the fatigue analysis using ASME best-fit curve is less conservative over high cycle region.

Table 5. Fatigue Lives of Test Specimens Obtained from Fatigue Test.

Case	Specimen Number	Fatigue Life Cycle	Average
1	1-1	2501	2478
	1-2	1340	
	1-3	3594	
2	2-1	26949	19979
	2-2	16079	
	2-3	16909	
3	3-1	800065	552947
	3-2	484176	
	3-3	374601	

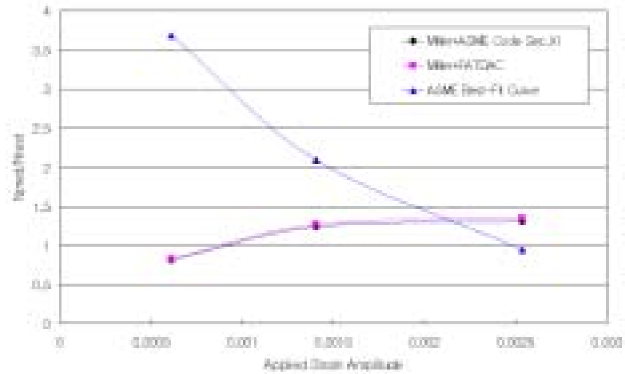

Fig. 9. Ratios of Predicted Fatigue Lives to Average Test Data

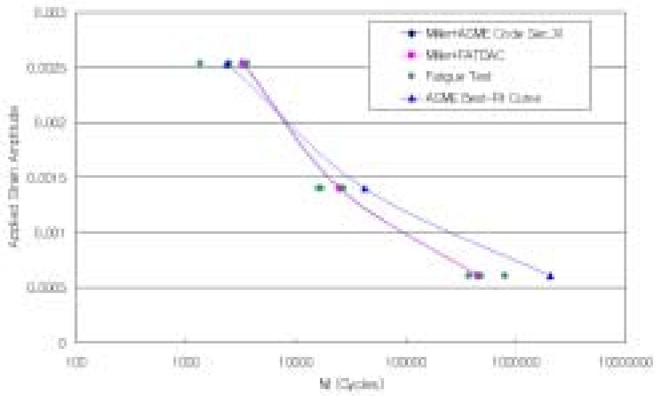

Fig. 10. Predicted $\Delta\varepsilon$-N_f Curves and Test Data.

6. CONCLUSIONS

A study on fatigue analysis procedure of nuclear welded structures was performed based on the structural stress/fracture mechanics approach. From this study, some major findings are obtained as follows:

● The modified mesh-insensitive structural stress procedure is proposed for reliable application to the welded joints with local thickness variation and inignorable shear/normal stresses along local discontinuity surface.
● The structural stress calculated from the modified structural stress procedure can serve as an intrinsic stress parameter because of the mesh-size insensitiveness.
● The structural stress/fracture mechanics approach agrees well with the fatigue test results over all cycle regions.

References

[1] J.M. Barsom and R.S. Vecchio, Fatigue of Welded Structures, Welding Research Council Bulletin 422, June, 1997.
[2] ASME Sec. XI TaskGroup on Fatigue Operating Plants, Metal Fatigue in Operating Nuclear Power Plants, Welding Research Council Bulletin 376, November, 1992.
[3] ASME B&PV Committee, 2000, ASME B&PV Code Section III.
[4] P. Dong, "Structural stress definition and numerical implemen-tation for fatigue analysis of welded joints," Int. J. of fatigue, Vol.23, pp.865-876, 2001.
[5] H. Adib and G. Pluvinage, "Theoretical and numerical aspects of the volumetric approach for fatigue life prediction in notched components," Int. J. of Fatigue, Vol.25, pp.67-76, 2003.
[6] P. Dong, J.K. Hong and Z. Cao, "Mesh-insensitive structural stress procedure for fatigue evaluation of welded structures,"Int. Institute of Welding, IIW Doc. XIII-1902-01/XV-1089-01, July, 2001.
[7] ASME B&PV Committee, 2000, ASME B&PV Code Section II.
[8] E. Niemi and P. Tanskanen, "Hot spot stress determination for welded edge gussets," IIW XIII-1781-99, 1999.
[9] M. Wagner, "Fatigue strength of structural members with in-plane notches," IIW Doc. XIII-1730-98, 1998.
[10] H.B. Park and O.K. Chopra, "A fracture mechanics approach for estimating fatigue crack initiation in carbon and low-alloy steels in LWR coolant environments," ASME PVP 2000, PVP-Vol.410-2, pp.3-11, 2000.
[11] J.C. Newman Jr., "The merging of fatigue and fracture mechanics concepts:

a historical perspective," Progress in Aerospace Science, Vol.34, pp.347-390, 1998.
[12] H. Tada, P. Paris and G. Irwin, The Stress Analysis of Cracks Handbook, 2nd Edn, Paris Productions Incorporated, St. Louis, Missouri, 1985.
[13] K. Tokaji, et al., "The growth of small fatigue cracks in low carbon steel; the effect of microstructure and limitation of linear elastic fracture mechanics,"Fatigue Frac. Eng. Mater, Struct., Vol.9, pp.205-217, 1986.
[14] K. Tokaji, et al., "Limitation of linear elastic fracture mechanics in respect of small fatigue cracks and microstructure,"Fatigue Frac. Eng. Mater. Struct., Vol.9, pp.1-14, 1986.
[15] D.J. Gavenda, et al., "Crack initiation and growth behavior of carbon and low-alloy steels," Fatigue and Fracture 1, PVP 350, ASME, pp.243-225, 1997.
[16] D. Taylor and J.F. Knott, "Fatigue crack propagation behavior of short crack; the effect of microstructure," Fatigue Frac. Eng. Mater. Struct., Vol.4, pp.147-155, 1981.
[17] N.E. Dowling, "Crack growth during low-cycle fatigue of smooth axial specimens," ASTM STP 637, pp.97-121, 1977.
[18] K.J. Miller, "Initiation and growth of short fatigue cracks,"Fundamentals of Deformation and Fracture, B.A. Balley, K.J. Miller and J.R. Willis, eds, Cambridge University Press, pp.477-500, 1985.
[19] P.D. Hobson, "The formation of a crack growth equation for short cracks," Fatigue Frac. Eng. Mater. Struct., Vol.5, pp.323-327, 1982.
[20] ASME B&PV Committee, 2000, ASME B&PV Code, Sec.XI, Article A-4300
[21] E.D. Eason, et al., "Analysis of pressure vessel steel fatigue test in air," Nuclear Engineering and Design, Vol.115, pp.23-30, 1989.
[22] O.K. Chopra and W.J. Shack, "Overview of fatigue crack initiation in carbon and low-alloy steels in light water reactor environments," J. of Pressure Vessel technology, Trans. of ASME, Vol.121, pp.49-60, 1999.